Economics Bulletin

Volume 44, Issue 1

Bayesian statistical inference addressed to share prices dynamics' theory

Geoffrey Ducournau
SEM, Tsinghua University; MRE, University of Montpellier; Dimtech

Daniel Melhem
Dimtech ; MRE, University of Montpellier

Abstract

This paper examines the Osborne' Brownian motion theory to prices dynamics. Osborne's assumption is modified to account for the asymmetry of opportunity due to agents' update of the probability of profit overtime. We provide numerical illustrations to demonstrate the underlying behavior of these dynamics by considering the change in prices under an assumed conservative system and a dissipative system. Under a conservative system, results showed that the dynamics quickly converge to a global equilibrium, which is the marginal probability of profit in a fair game. Under a dissipative system, the dynamics can be described by a superposition of distributions in local equilibrium with constant variance satisfying locally the implications of Osborne's theory. Globally, the dynamics do not reach equilibrium, and its distribution exhibits asymmetries of opportunity and is characterized by a changing variance. We finally extend our work and provide empirical evidence that the variance dynamism of the S&P500 index undergoes statistical transition from high to low timeframe. Under high frequency, the lognormal and inverted gamma distributions best explain the variance dynamism; under low frequency, the gamma distribution best explains it. This conclusion paves the way to a new approach to volatility modeling and asset pricing by considering stock returns dynamics as a superposition of statistics with known mean and unknown variance, namely a superstatistics.

Paper #8 in Special issue "In memory of Pr. Michel Terraza" Geoffrey Ducournau, SEM, Tsinghua University; MRE, University of Montpellier; Dimtech G.ducournau.voisin@gmail.com Daniel Melhem, PhD, Dimtech ; MRE, University of Montpellier Daniel.melhem@111dimtech.com
Citation: Geoffrey Ducournau and Daniel Melhem, (2024) "Bayesian statistical inference addressed to share prices dynamics' theory", *Economics Bulletin*, Volume 44, Issue 1, pages 373-398
Contact: Geoffrey Ducournau - g.ducournau.voisin@gmail.com, Daniel Melhem - daniel.melhem@111dimtech.com.
Submitted: August 23, 2021. **Published:** March 30, 2024.

EB Economics Bulletin

Picture credits: Virginie Terraza

Special issue "In memory of Professor Michel Terraza"

1. Introduction

Osborne (1959) Brownian motion theory of share prices dynamics relies on the assumption of perfect symmetry of opportunity of profit between financial agents and implies that over nonoverlapping intervals of time, this symmetry is maintained and share prices dynamics constitute a random walk defined by a common probability function with constant variance. To reach this conclusion, Osborne made fundamental assumptions that we summarize into five points.

The first assumption results in considering the logarithm of prices as the appropriate ratio to measure the change in prices. If $p(t)$ represents the price of a share at time t, then $x = \ln(p_{t+\tau}) - \ln(p_t)$ is the change in the log of price from time t to $t + \tau$. Osborne considers that the subjective feeling from change in prices addressed to financial agents is best explained by the Weber-Fechner Law (Norwich 1987, Maes 2021).

The second assumption results in considering prices as an ensemble of molecules in equilibrium in statistical mechanics. The probability distributions of the steady state is determined by the condition of maximum probability and the equilibrium distribution is given by:

$$P(x) = \frac{1}{\sqrt{2\pi\sigma^2}} e^{-x^2/2\sigma^2} \tag{1}$$

where σ^2 is the variance of x and the mean is considered as null. Consequently, the distribution is the same as that of a particle in Brownian motion.

The third assumption consider the variance σ^2 of price changes as constant over unit time interval.

The fourth assumption result in defining the conditions under which a financial agent is most likely to bet on the market. Osborne argues that the most probable condition under which a transaction on the share price market is possible is obtained when the expected opportunity of profit from the seller and the buyer on each bet are maximized and in the long term are equal. In other words, in the long term, the sum of the Buyer and Seller's expected profit is null, and the time necessary to reach this equilibrium is determined by a finite variance which increase at the square root of number of times.

This "symmetry of opportunity" as assumption has been examined and questioned in several studies and authors, including Osborne (1959) himself, Fama (1965) and most recently Logfren (2002) by emphasizing certain evidence that asymmetric information was a common feature and necessary conditions of market interactions. One consequence with Osborne's theory is that financial agents are homogeneous, share the same common information and, therefore, take the decision to bet or not on the market according to an identical decision process.

We propose in this article to keep the same assumption by considering that financial agents take a decision if and only if it maximizes their opportunity of profit given their available information. We define the information available to agents as their probability of profit conditioned on their historical series of outcomes on previous bets. In other words, we consider that each agent updates his or her expected opportunity of profit through Bayesian inference taking each new outcomes as new and additional information vis-à-vis their current state. Consequently, agents can be seen as a group of local homogeneous agents sharing identical information (i.e., same conditional probability of profit), and the system as constituting of an ensemble of heterogeneous groups (i.e., groups of agents with different conditional probabilities of profits), also called coarse-grained. Considering these heterogeneities of opportunity of profit between agents, we seek to understand the implication of this phenomenon on the distribution of the share price dynamics and its eventual underlying complex behaviors characterized among other by asymmetries, heavy tailed or even power law decay. To this end, we perform numerical simulations of share price dynamics distribution considering this last whether as a conservative system, whether as a dissipative system.

In the first section, we perform numerical simulations on these two experimental scopes and show statistical evidence of asymmetry in opportunity of profit in the long term. In the second section, we show evidence that Bayesian inference gives a theoretical solution to the numerical assessment made in the first section. We demonstrate that these asymmetries come from an underlying statistic governing the system's volatility dynamics. Further, we show empirical evidence that these volatility dynamics change based on the time frequency studied.

2. Numerical experimentations

We compute a numerical model to study the dynamics of log returns by simulating changes in opportunity of profit among financial agents. Under Osborne 'assumptions, if the long-term average opportunity of profit of the system converges to 0.5 (i.e., marginal probability of profit on a single bet), then the long term means of log returns converge to 0 with a significant symmetry within its distribution due to agents' homogeneity of opportunity. We test these assumptions under two experimental scopes:

- Considering prices dynamics as a conservative system. The system is isolated with no interactions with its surrounding. The system starts and end with the same number of financial agents.
- Considering prices dynamics as a dissipative system. The system interacts with its surrounding, enable new agents to entry the market, and agents to exit if they consider having a too low opportunity of profit or if they bankrupt.

2.1. Conservative system

We consider the system constituting an ensemble of financial agents as a macro-state Ω where each agents decides to bet based on a set of given information. We describe each agent as a micro-state $\mathcal{M}_i$ of Ω with given probability of profit $p_{\mathcal{M}_i}$, where $i = 1, \dots, n$, with n the number of micro-states. This number is fixed and will remain the same until the end of the experiment (conservative system). Initially, we assume, as Osborne, that agents are homogenous and share the same opportunity of profit. However, as the bets proceed, each agent updates their probability of profit according to their previous series of outcomes. Thus, maximizing their opportunity of profit relies on maximizing their posterior probability of observing a profit on their next bet given the historical outcomes:

$$P(win|\mathcal{M}_i) = \frac{P(win) * P(\mathcal{M}_i|win)}{P(win) * P(\mathcal{M}_i|win) + P(loss) * P(\mathcal{M}_i|loss)} \quad (2)$$

Where $\mathrm{P(win)} = \mathrm{P(loss)}$ is the marginal probability of profit and loss.

Figure1 (appendix A) provide a simplified illustration of the numerical simulation. We have six successive macro-states in which a transaction between at least two micro-states occurs. Each macro-state constitutes five independent micro-states {A, B, C, D, E}, and we assume in step 1 that the Osborne condition holds (i.e., homogeneity of opportunity of profit between micro-states). Figure 1 must be read by following the arrays so that the transaction occurring in step 1 is followed by the transaction occurring in step 2, and so on.

We represent the posterior probability using a given color. If the color is the same for different micro-states, it means they are homogeneous. The color of micro-states changes with each step because each micro-state updates their posterior probability according to the last bet's outcome. Table 1 (appendix A) emphasizes this evolution in the posterior probability for each micro-states as the bets progress over time.

The numerical simulation is based on the same logic. We start with 750 micro-states that initially have the same probability of profit. At each iteration, at least one bet between two micro-states occurs leading to an update of their respective posterior probability of profit. We run the model for 10,000 iterations and determine, for each iteration, the smoothing average of the macro-state posterior probability of profit, the macro-state posterior probability distribution, the macro-state entropy evolution, and finally the evolution of posterior probabilities of each micro-state. The macro-state that defines the system equilibrium is the one with the most identical microstates, namely the highest entropy. In other words, the more the system is constituting of microstates with equal probability of profit, the more the system tends to converge to its equilibrium and maximize its entropy.

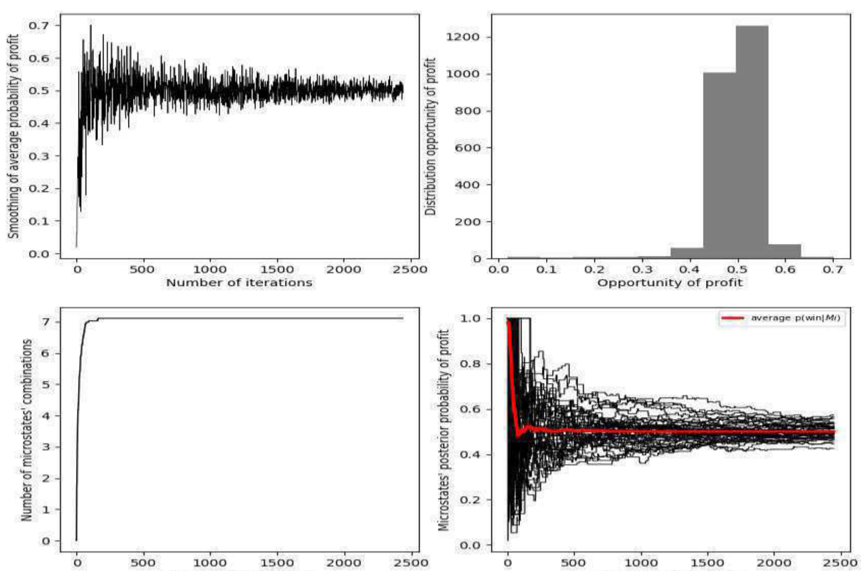

Figure2: Experiment under conservative system hypothesis. Upper left plot: smoothing average of the macro-state posterior probability of profit. Upper right plot: macro-state probability of profit distribution. Lower left plot: evolution of number of microstates with marginal probability of 0.5. Lower right plot: evolution in microstates' posterior probability of profit.

Figure2 emphasizes statistical outcomes from the first experiment. The distribution of opportunity of profit is highly concentrated around its mean, roughly equal to 0.5, meaning that over time, the average probability of profit of the system converges to a marginal probability of profit of a fair game. We make the same assessment on the evolution of microstates' opportunity of profit. Over time, they all converge to 0.5. The marginal probability of profit is reached when the number of microstates with equiprobability of profit has reached its maximum, meaning the entropy of the system is maximized. As expected, due to the heterogeneity of available information between microstates (i.e., information depends on previous bets' outcomes), we assess asymmetries within the distribution of opportunity of profit. In Table2, we determine the asymmetry by measuring the skewness of the distribution. We measure a skewness of -1.45, which contradict Osborne's theory of perfect symmetry and equilibrium being reached when the data converges to a normal distribution. However, a kurtosis of 3.21 indicates that the distribution is not far from being platykurtic, producing little outliers.

Table2: Statistical outcomes from simulated data and its distribution (Conservative system).

Simulated data	Mean	Median	Skewness	Kurtosis
Opportunity of profit	0.468	0.487	-1.45	3.21

We have compared the data to other distributions by fitting the data to the normal distribution, the t-student distribution, the Cauchy distribution, the Pearson distribution, and Laplace distribution. We use these distributions because, as Mandelbrot (1969) and Fama (1963), we assume that distributions that represent price changes are intermediate between a Cauchy and a normal distribution. Figure3 & Table3 show our results. We compare all distributions by using the sum of square errors and show evidence that the t-student distribution should be preferred to explain the dynamics of opportunity of profit between agents. We computed a parametric bootstrap p-value with 5% significance level. The results are unanimous: among all distributions tested, the t-students distributions remain the best fit with the highest p-value converging towards 0.429. We show that we cannot reject the null hypothesis that the distribution of opportunity of profit is normally distributed. Results are shown in Table3 and Figure13 (AppendixA).

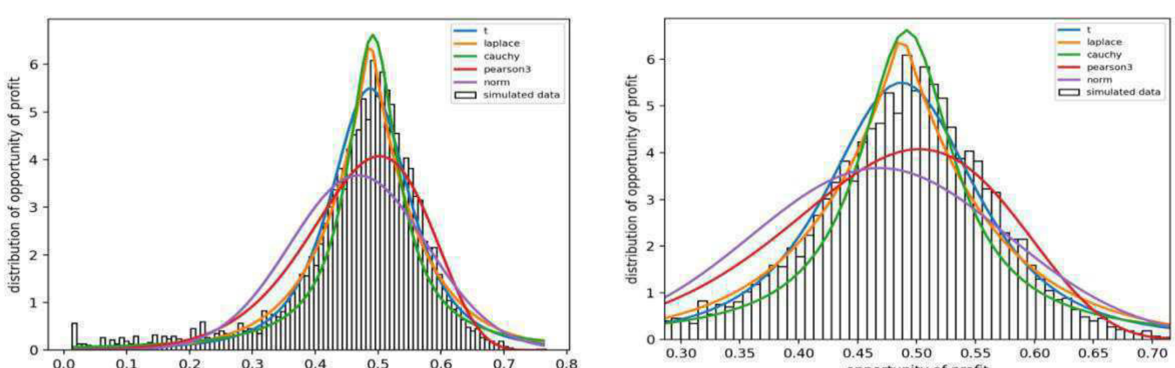

Figure3: Conservative System. Left: distribution of the opportunity of profit under different discrete binning and different statistics (blue: t-students, yellow: Laplace, green: Cauchy, red: Pearson and purple: norm). Right: same plot but scaled-up.

Table3: Distributions model comparison with sum of squared errors methodology. The distribution model that fits the simulated data with the lowest SSE should be preferred.

Distribution model	SSE	aic	P-value	Parameters fitting
t-student	7.80	172.95	0.0429	υ: 2.72, μ: 0.49, σ: 0.66
Laplace	12.80	159.65	0.284	μ: 0.49, σ: 0.75
Cauchy	19.42	141.01	0.29	μ: 0.49, σ: 0.048
Pearson	27.92	245.10	0.387	υ: −0.66, μ: 0.47, σ: 0.10
Normal	57.02	197.07	0.127	μ: 0.47, σ: 0.11

2.2. Dissipative system:

We have previously considered the system as closed, constituting a fixed number of financial agents. We now consider the system as coarse-grained, constituting an ensemble of groups of homogenous financial agents interacting with other heterogenous groups. The system is also dissipative, enabling new financial agents to enter or exit the system. We also consider the inflow and outflow of agents as time independent, leading to spatiotemporally inhomogeneous dynamics. Figure4 in appendix A proposes an illustration in which the simulation model is built up. We consider the macro-state Ω constituting an inhomogeneous ensemble of local macro-states $(\omega_1, \omega_2, \omega_3 \dots \omega_N)$, more or less heterogeneous, interacting with each other, constituting respective microstates of different sizes such as $\mathcal{M}_1 \subset \omega_1$ and $\mathcal{M}_1 = \{\mathcal{M}_{1i}\}$ with $i = 1, \dots, n_1$; n_1 corresponds to the number of microstates $\mathcal{M}_1$. We consider this representation as more realistic than the conservative system. In this experiment, financial agents update their opportunity of profit according to the same inference described in the previous experiment.

The numerical simulation models the dynamics of four local macro-states ω_N (N= 4) constituting, respectively, 750, 225, 150 and 425 microstates. The number of microstates is an arbitrary choice and has no impact on the overall dynamics, only on its speed of convergence to the equilibrium. These microstates are not simultaneously interacting with the system but interact with different time intervals. Consequently, each microstate updates their probability of profit with different speed. As in the previous experiment, we ran the model for 10,000 iterations and illustrate the simulation's outcomes in Figure5. We show that the system dynamics are a superposition of different local statistics corresponding to the respective local-macro-state behavior. Each local-macro state converges to the same marginal probability of profit of 0.5, but with different speed. This speed of convergence depends on the number of interactions with the system and, consequently, with the number of microstates that constitute it. The larger the number of microstates, the slower the convergence.

Moreover, this different speed in dynamics leads to more asymmetries in the system's distribution of opportunity of profit because it exacerbates its heterogeneity characteristic. Table4 provides statistics regarding the simulated data. The kurtosis is equal to 9.11 and the skewness is equal to -2.33, both being much greater than under the previous experiment. This corresponds to a leptokurtic distribution with greater extremity of deviations with more data far from the system equilibrium. Consequently, the distribution tails approach zero more slowly than under a Gaussian distribution, producing more outliers than the normal distribution and contradict Osborne's theory.

We add that this simulation is a simplification of real market heterogeneities and degrees of freedom, meaning that if we were able to simulate the changes in opportunity of profit of real financial agents, we may observe a distribution much further away from equilibrium and with more asymmetries.

Table4: Statistical outcomes from simulated data and its distribution (Dissipative system).

Simulated data	Mean	Median	Skewness	Kurtosis
Opportunity of profit	0.485	0.496	-2.33	9.11

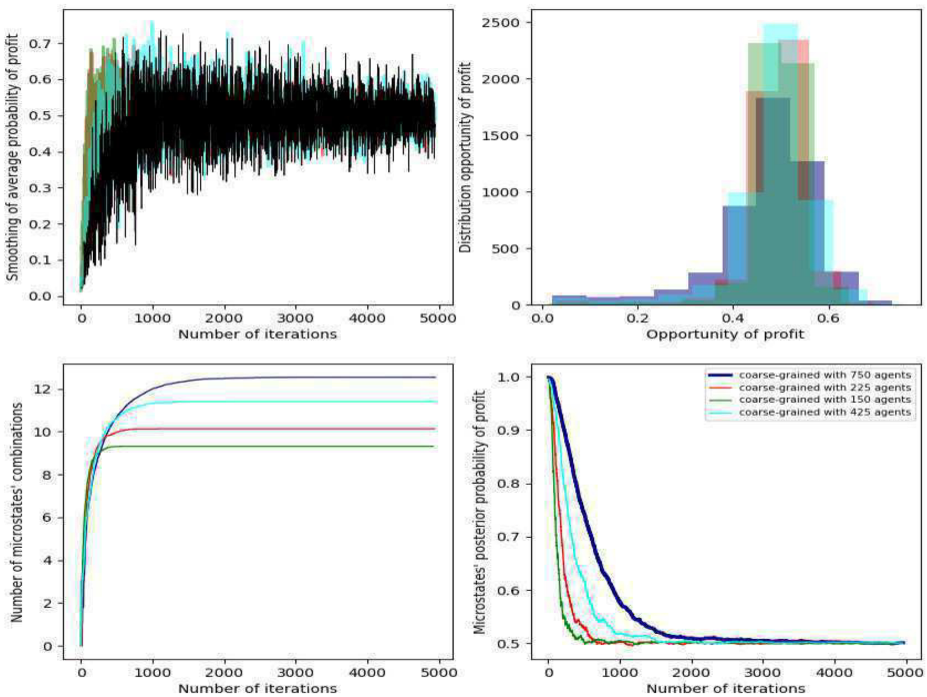

Figure5: Experiment under dissipative system hypothesis. Upper left plot: smoothing average of the local macro-states (coarse-grained) posterior probability of profit. Upper right plot: global macro-state probability of profit distribution. Lower left plot: evolution of number of microstates with marginal probability of 0.5. Lower right plot: evolution in local macro-states posterior probability of profit.

Figure6 & Table5 show the results of the comparison between the simulated data and the normal distribution, the t-student distribution, the Cauchy distribution, the Pearson distribution, and Laplace distribution. As in the previous experiment, we compared all distributions using the sum of square errors and show evidence that the t-student distribution should be preferred to explain the dynamics of opportunity of profit between agents, i.e., the change in log-returns. We computed a parametric bootstrap p-value with 5% significance level. The results are unanimous: among all distributions tested, the t-students distributions remain the best fit with the highest p-value converging towards 0.466. We also reject the null hypothesis that the distribution of opportunity of profit is normally distributed. Results are shown in Table5 and Figure13 (AppendixA).

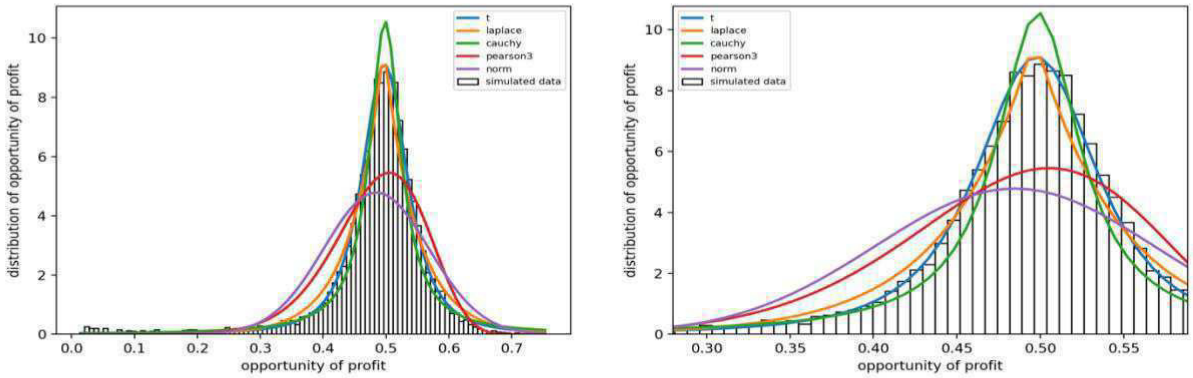

Figure6: Superposition of local macro-state distribution from a dissipative system. Left: distribution of the opportunity of profit under different discrete binning and different statistics (blue: t-students, yellow: Laplace, green: Cauchy, red: Pearson and purple: norm). Right: same plot but scaled-up.

Table5: Distributions model comparison with sum of squared errors methodology. The distribution model that fits the simulated data with the lowest SSE should be preferred.

Distribution model	SSE	aic	P-value	Parameters fitting
t-student	2.77	283.36	0.466	$\upsilon: 2.12, \mu: 0.50, \sigma: 0.04$
Laplace	13.42	339.35	0.08	$\mu: 0.49, \sigma: 0.05$
Cauchy	20.69	206.17	0.348	$\mu: 0.50, \sigma: 0.03$
Pearson	91.28	575.71	0.398	$\upsilon: -0.54, \mu: 0.48, \sigma: 0.076$
Normal	142.78	496.66	0.018	$\mu: 0.48, \sigma: 0.083$

We show that as soon as the system becomes less dissipative[1] with less heterogeneous microstates interacting, each local macro-state will converge towards the equilibrium probability of profit of 0.5. Consequently, the speed of convergence of the system will depend on its degree of dissipation that we can think of as the amount of liquidity, the volume of transactions, and a fortiori the number of heterogenous financial agents interacting in the market. We also show that the posterior probability of profit of each local macro-state does not evolve under the same dynamics. Some also converge faster to their equilibrium state. This is due to the fact that, in our model, each local macro-state and a fortiori microstates do not share the same information and, therefore, do not update their probability of profit according to the same dynamics. One consequence is that each local-macro state is defined by a respective distribution of opportunity of profit with its respective variance, as shown in Figure7 and Table6. Figure14 (Appendix A) gives respective p-values results from the goodness of fit test and shows that the t-students distributions remain the best on every local macro-state distribution.

[1] Because we cannot run the model with infinite number of new local macro-states, as the iterations go, the system becomes more conservative since there are less interactions with new microstates.

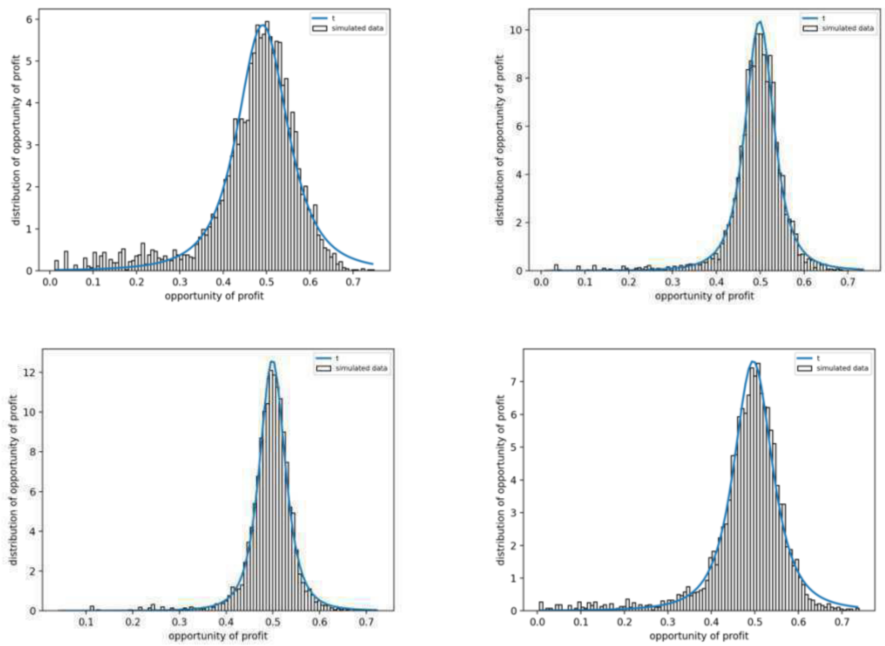

Figure7: Probability distribution of individual local macro-state with t-students fitting. Upper left: coarse-grained ω_1 with 750 microstates. Upper right: coarse-grained ω_2 with 225 microstates. Lower left: coarse-grained ω_3 with 150 microstates. Lower right: coarse-grained ω_1 with 425 microstates.

Table6: Local macro-states statistics and t-student fitting outcomes.

Distribution model	Mean, variance	skew	kurtosis	t-student fitting	SSE
$\omega_1 = 750\ agents$	$\mu: 0.47, \sigma^2 : 0.011$	-1.5	3.25	$\upsilon: 2.48, \mu: 0.49, \sigma: 0.06$	10.45
$\omega_2 = 225\ agents$	$\mu: 0.49, \sigma^2 : 0.005$	-2.43	11.98	$\upsilon: 2.51, \mu: 0.49, \sigma: 0.03$	11.06
$\omega_3 = 150\ agents$	$\mu: 0.47, \sigma^2 : 0.011$	-2.31	13.35	$\upsilon: 2.75, \mu: 0.49, \sigma: 0.029$	6.88
$\omega_4 = 425\ agents$	$\mu: 0.48, \sigma^2 : 0.008$	-2.01	6.82	$\upsilon: 2.38, \mu: 0.49, \sigma: 0.047$	7.35

If taken individually, every local macro-state may not describe a significant leptokurtic distribution similar to the conservative experiment. Globally, the distribution of the system consists in a superposition of statistics with different variance and a known mean converging over time to a marginal probability of profit. We posit that this fluctuating variance at a global scale is the cause of more asymmetries and excess of kurtosis within the observed distribution (Figure6).

Finally, under a dissipative system, there is enough evidence to reject the normal distribution proposed by Osborne with perfect symmetry of profit between agents. Moreover, due to the superposition of statistics, we show that the other major assumption in the derivation of Osborne's model regarding a constant variance of price changes is not valid. We show in our experiment that σ^2 represents the degree of activity from financial agents' interactions and varies according to space and time. This fluctuating variance at global scale due to superposition of statistics is the extension we wish to analyze in the next section. We consider that the variance of share price changes is a random variable with distribution $g(\sigma^2)$, and we will show [that this last transit] from different types of statistics according to time frequency.

3. Empirical evidence of transitory stochastic volatility

We consider now the variance of share price changes as a random variable with distribution function $g(\sigma^2)$. Consequently, the distribution given by Osborne in equation (1) must be reinterpreted as a conditional probability distribution given the variance σ^2 such that equation (1) becomes:

$$P(x|\sigma^2) = \frac{1}{\sqrt{2\pi\sigma^2}} e^{-x^2/2\sigma^2} \tag{3}$$

And P(x) becomes the probability distribution of x, which takes into account the random nature of σ^2 such that we obtain P(x) by solving the following equation:

$$P(x) = \int_0^{\infty} P(x|\sigma^2) * g(\sigma^2) d\sigma^2 \tag{4}$$

with $0 \leq \sigma < \infty$. In equation (4), $g(\sigma^2)$ represents a prior distribution for the unknown parameter σ^2. As already discussed by Raiffa and Schlaifer (1961), an effective approach to determine the dynamics of σ^2 is a Bayesian alternative where the likelihood of $P(x|\sigma^2)$ is defined by a standard normal distribution of known μ and unknown σ^2 where the conjugate prior of $g(\sigma^2)$ for a sample assumed normally distributed is theoretically accepted as being an inverted gamma distribution defined by equation (9) (Appendix B) (Liu & Wasserman, (2014)). We also assume that having a prior on the mean μ is not necessary since, from our experiments, we show its convergence to equilibrium leading to a long term mean of log returns converging to zero. Deyer (1976) show empirical evidence that the variability of log return means was not as strong as the variance. More recent studies from Ma and Serota (2014) show it is theoretically possible that other prior distribution exist to describe σ^2, including inverse gamma (IGa), lognormal (LN), gamma (Ga), and the generalized inverse gamma (GIGa) distribution, all belonging to the same family of distributions. They also conclude that the Student's t-distribution provides one of the better fits to log returns of S&P component stocks and argue that stock returns can be understood as the product distribution of volatility and normal distributions.

Their conclusions are consistent with the conclusions drawn from both of our experiments and reinforce the Bayesian Inference alternative to model the variance distribution. However, in their work, Tao Ma and R.A. Serota do not study the dependence of the variance distribution on time frequency. If the distribution function $g(\sigma^2)$ represents the changing expectations of opportunity of profit of group of agents (i.e., *in fine* the expected returns), we can assume that the nature of this function may change according to time since the degree of opportunities are also varying.

We propose to analyze the volatility distribution function $g(\sigma^2)$ of the Standard&Poor500 from January 01, 2016 to July 16, 2021 according to four different time scales i.e., minutes, daily, weekly and monthly, and according to three prior models i.e., LN, IGa and Ga. We do not consider the GIGa model since it is directly related to LN, IGa and Ga according to the parameters β and γ. In other words, LN, IGa and Ga are special cases of GIGa.

By considering the mean parameter μ as equal to zero, we calculate the variance by squaring the log returns. Figure8 illustrates the time series used for this study on a minute time frame (figures on other time frame are shown in figure15 from Appendix C).

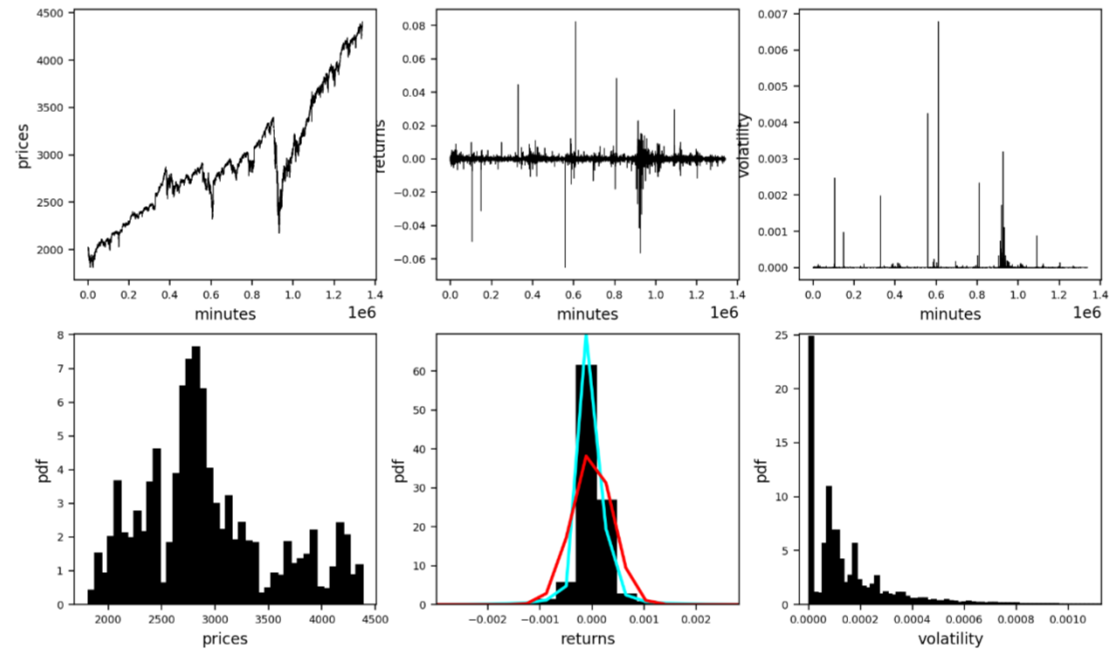

Figure8: Standard&Poor500 time series with minutes time frame from January 01, 2016 to July 16, 2021. Upper left: Standard&Poor500's prices with minutes time frame. Upper middle: Standard&Poor500's Log returns. Upper right: Standard&Poor500's prices volatility. Lower left: Distribution in percentage of Standard&Poor500's prices. Lower middle: Distribution in percentage of Standard&Poor500's Log returns. The cyan color line is a fit of t-students distribution. The red color line is a fit of normal distribution. Lower right: Distribution in percentage of Standard&Poor500's volatility.

We then minimize the negative likelihood with Bayesian optimization using Gaussian Processes method to estimate the best fitting parameters of IGa, LN and Ga. The parameters of fitting distributions results with minutes data are summarized in Table7 (results for the other time frames are shown in Table10 from appendix D). Figure16 (appendix D) compares the likelihood of each distribution under different time frames. We show that the goodness of fit from LN, IGa and Ga increases as time frequency increases.

Table7: Parameters of fitting distribution on data with minutes time frame.

Minutes Data	2016	2017	2018	2019	2020	2021
IGa(x,α β)	α:1.98, β:4.18e-08	α:1.97, β:1.30e-08	α:1.97, β:3.25e-10	α:1.97, β:2.44e-08	α:0.468, β:3.52e-09	α:1.97, β:2.42e-08
LN(x,μ,σ)	μ: -5.40e-25 σ: 6.12	μ:-5.07e-24 σ:9.332	μ:-9.071e-28 σ: 6.624	μ:-1.49e-30 σ: 12.25	μ:-1.224e-22 σ: 10.61	μ:-8.22e-27 σ: 9.936
Ga(x,α,β)	α:2.96, β:0.793	α:0.00015, β:0.815	α:0.00033, β:0.815	α:7.096e-05, β:0.815	α:7.776e-05, β:0.793	α:0.000187, β:0.8148

We then compare each distribution fitness to the data using the sum of squared errors (SSE) methodology. The distribution model that fits the simulated data with the lowest SSE should be preferred. Results of the best fit distribution for the year 2016 are shown in Table8 (results for other years are shown in Table11 from Appendix D). In Figure10, we plot the empirical data distribution (i.e., Standard&Poor500 volatility) fitted with the best distributions among IGa, LN and Ga in 2016 and with their respective p-values (results for other years are shown in Figure17 and Figure18 from Appendix D). Table8,11 and Figure10,17&18 shows that there is a transition of statistics from high to low frequency time frame. Using high frequency data (i.e., minutes), the LN statistic fit the data better. Using lower frequency data (daily), we assess a mixture of statistics, with LN and IGa being the best candidates. Finally, using low frequency data (weekly and monthly), we show a clear transition of statistics towards a Ga distribution.

Table8: Distribution's fitting comparison with sum of squared errors methodology for the year 2016 and using different time frames. The distribution model that fits the simulated data with the lowest SSE should be preferred. In 2016, the model LN provides the best fit using minute and weekly data. The IGa model provides the best fit using daily data and the Ga model provides the best fit using monthly data.

Year 2016	**minutes**	**Daily**	**weekly**	**monthly**
Best fit distributions	**LN(x,μ,σ)**	**IGa(x,α β)**	**LN(x,μ,σ)**	**Ga(x,α,β)**
SSE from LN	**1.57e+09**	1.53e+08	**5.93e+07**	1.44e+08
SSE from IGa	1.64e+09	**1.12e+08**	1.38e+08	1.62e+08
SSE from Ga	1.63e+09	8.75e+08	6.29e+07	**1.11e+08**
p-value on best fit	0.173	0.0631	0.532	0.350

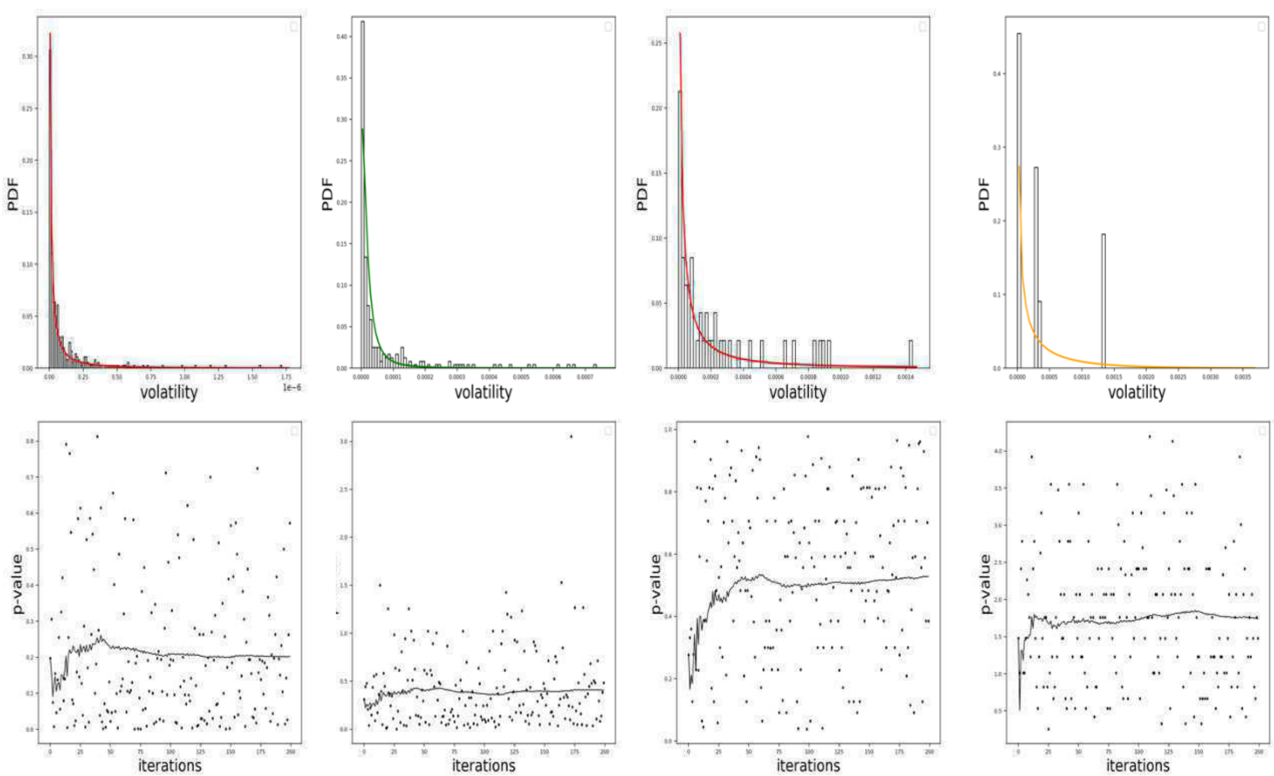

Figure10: On both upper & lower graph, from left to right, time frame = minutes, daily, weekly, monthly. Upper graph: empirical distribution plotted against best fit distribution. Red line corresponds to LN distribution, green line corresponds to IGa distribution, and yellow line corresponds to Ga distribution. Lower graph: Parametric Bootstrapping of p-value with Kolmogorov-Smirnov goodness of fit test regarding the best fit distribution.

4. Conclusion

In this paper, we demonstrate that share prices dynamics result from the interactions between financial agents defined by their respective opportunity of profit. We assumed that financial agent's decision making in respect of placing bets relies on updating their respective opportunity of profit via Bayesian inference and is conditioned to outcomes from previous bets. We proposed numerical experiments to illustrate the underlying behaviors of this dynamic by considering the share price changes under both a conservative system and a dissipative system.

Under a conservative system, we demonstrated that the overall opportunity of profit converges towards a fair game's marginal probability of profit, i.e., 0.5, confirming one of Osborne's assumptions. We also measure slight asymmetries of opportunity of profit and demonstrated that, although we cannot reject the normal distribution using the p-value, the t-student distribution is the optimal distribution to fit the simulated data. We contradict Osborne's theory of perfect symmetry of opportunity of profit between agents and show that equilibrium is reached when the data converges to a normal distribution.

Under a dissipative system, we consider the system as an ensemble of inhomogeneous and coarse-grained in interaction with its surrounding. Results from numerical simulations show that the system dynamics can be considered as a superposition of local statistics, all converging towards equilibrium (i.e., converging towards a probability of profit of 0.5) but under different speeds and different dynamics. This difference of speed in dynamics leads to asymmetries in the system's distribution of opportunity of profit and, at global scale, the system tends to equilibrium but does not reach it. From the simulated data, we show empirical evidence of a leptokurtic distribution with greater extremity of deviations, with more data far from the system equilibrium. We also reject by p-value the normal distribution and show that the t-student fits the data best. We reject Osborne's theory of perfect symmetry of opportunity between agents, reject the normal distribution, and reject the hypothesis of constant variance. Indeed, the superposition of statistics indicates that, at global scale, the system dynamics is characterized by fluctuating volatility depending on space and time.

We then argue that stock volatility should be seen as a random variable with distribution $g(\sigma^2)$. We also provide theoretical evidence that, via Bayesian Inference, under the assumption that the likelihood has time to converge to a Gaussian process, the distribution $g(\sigma^2)$ is an inverse gamma distribution.

Lastly, we demonstrated that other prior distributions such as the lognormal and the gamma distribution to describe the variance dynamism should be taken into consideration depending on the study timescale. Indeed, we provided empirical evidence using the Standard&Poor500 that the variance dynamism undergoes statistical transition from high to low time frequency. Under high time frequency (i.e., minutes), the lognormal distribution best fits the σ^2. Under a daily timeframe, we observe a mix of statistics between the inverted gamma and lognormal distribution as the best fit distributions. Using low time frequency data (i.e., weekly, monthly), we observe a clear transition of σ^2 towards a gamma distribution.

These are important observations as the dependence of σ^2 on the data timeframe can explain other statistical phenomenon such as long-range persistence. Indeed, since it is well known that the lognormal and the inverted gamma distribution accounts for the power law tails, we also know that the gamma distribution cannot generate power-law tail.

Finally, these results can lead to better approaches for modeling volatility according to a given study time frame and can open the way to developing alternative volatility models.

References

Dyer, J.C., (1976) “Random walk in Australian share prices: a question of efficient capital markets”, *Australian economic papers*, (**15 (27)),** p.186-200.

Fama, E., (1965), “The Behavior of Stock Market Prices”, *Journal of Business* **(38)** :34-105.

Fama, E., (1963) “Mandelbrot and the stable Paretian hypothesis”, *Journal of Business*, **(36)**:420–429.

Liu, H., Wasserman, L., (2014) “Statistical Machine Learning”, Chapter 12 – Bayesian Inference, p302, p.303, p.311, p.312, p.315.

Logfren, K.G., Persson, T., Weibull, J.W., (2002) “Markets with Asymmetric Information: The Contributions of George Akerlof, Michael Spence and Joseph Stiglitz”, Scand. *Journal of Economics* **(104(2))**, 195-211

Maes C., (2021) “Statistical mechanical foundation of Weber-Fechner laws”, *Journal of Statistical Mechanics* **182**, 12pp, DOI: 10.1007/s10955-021-02726-0

Ma, T., Serota, R.A., (2014) “A model for stock returns and volatility”, *Physica A: Statistical Mechanics and its Applications*, (**398**), Pages 89-115.

Mandelbrot, B., (1969) “Long-Run Linearity, Locally Gaussian Process H-spectra and Infinite Variance”, *International Economic Review* (**10)**: 82-111.

Norwich, K.H., (1987) “On the theory of Weber fractions”, University of Toronto, Ontario, Canada, Perception & Psychophysics, **(42 (3))** 286-298

Osborne, M.F.M., (1959) “Brownian motion in the stock market”, US Naval Research Laboratory, Washington DC (**25)**.

Raiffa, H., Schlaifer, R., (1961) “Applied statistical decision theory”, Division of Research, Graduate School of Business Administration, Harvard University, ISBN: 0875840175, 9780875840178

Appendix A: Numerical Experimentations and statistics results

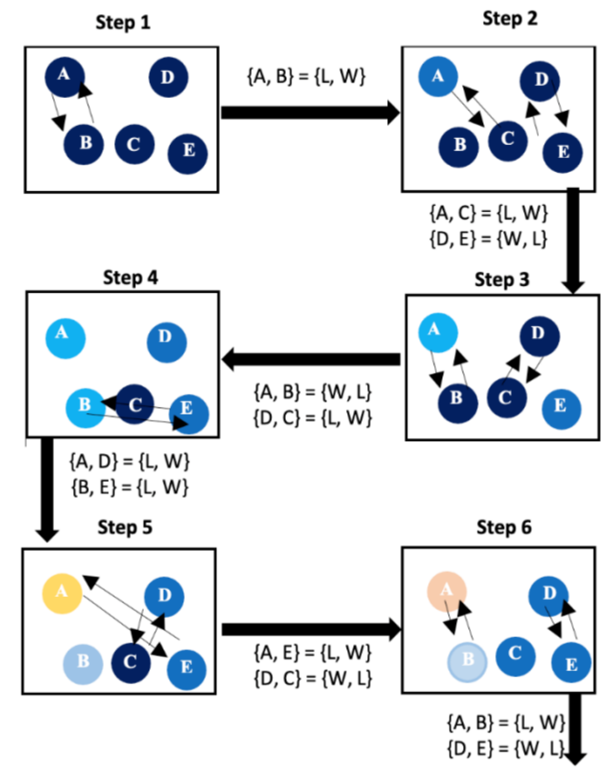

Figure1: Simplified illustration of the numerical simulation under conservative system. At each step at least one bet occurs between two microstates. In step1, A bets against B, A loose and B win. A and B update their probability of profit in a Bayesian way.

Table1: Posterior probability evolution of each micro-states as the bets progress over time.

Step 1	**A**	**B**	**C**	**D**	**E**	
Win	1	1	1	1	1	5
loss	0	0	0	0	0	0
P(win|$\mathcal{M}_i$)	1	1	1	1	1	1
Step 2	**A**	**B**	**C**	**D**	**E**	
Win	1	2	1	1	1	6
loss	1	0	0	0	0	1
P(win|$\mathcal{M}_i$)	0.5	1	1	1	1	0.9
Step 3	**A**	**B**	**C**	**D**	**E**	
Win	1	2	2	2	1	8
loss	2	0	0	0	1	3
P(win|$\mathcal{M}_i$)	0.16	1	1	1	0.27	0.69
Step 4	**A**	**B**	**C**	**D**	**E**	
Win	2	2	3	2	1	10
loss	2	1	0	1	1	5
P(win|$\mathcal{M}_i$)	0.33	0.5	1	0.5	0.33	0.53
Step 5	**A**	**B**	**C**	**D**	**E**	
Win	2	2	3	3	2	12
loss	3	2	0	1	1	7
P(win|$\mathcal{M}_i$)	0.28	0.37	1	0.6	0.54	0.56
Step 6	**A**	**B**	**C**	**D**	**E**	
Win	2	2	3	4	3	14
loss	4	2	1	1	1	9
P(win|$\mathcal{M}_i$)	0.24	0.39	0.66	0.72	0.66	0.53
Step 7	**A**	**B**	**C**	**D**	**E**	
Win	2	3	3	5	3	16
loss	5	2	1	1	2	11
P(win|$\mathcal{M}_i$)	0.22	0.51	0.67	0.77	0.51	0.54

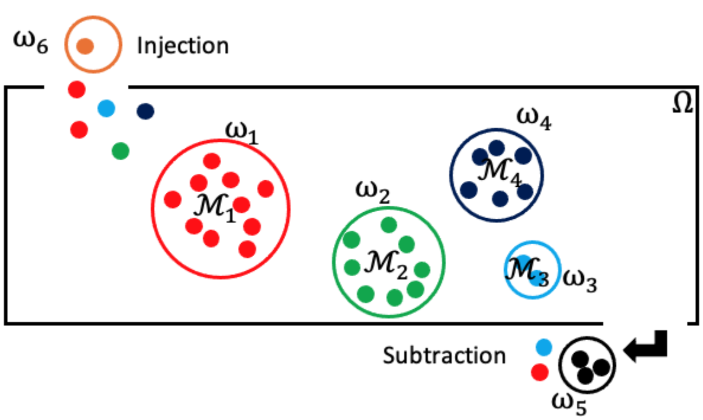

Figure4: Simplified illustration of the numerical simulation under dissipative system. Dissipative macro-state Ω with coarse-grained constituents $(\omega_1, \omega_2, \omega_3 \dots \omega_N)$ interacting between each other.

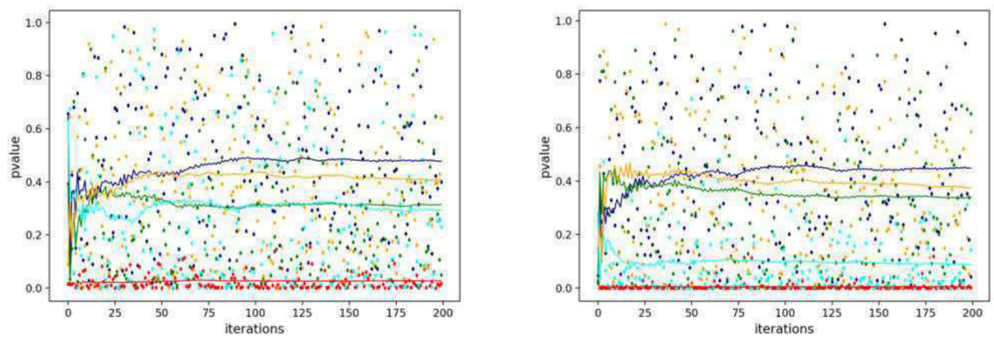

Figure13: Parametric Bootstrapping of p-value with Kolmogorov-Smirnov goodness of fit test. Left: p-values of fitting distribution on data from conservative system Right: p-values of fitting distribution on data from dissipative system; (blue: p-values from t-students' statistics, yellow: p-values from Laplace statistics, green: p-values from Cauchy statistics, red: p-values from normal statistics, cyan: p-values from Pearson statistics).

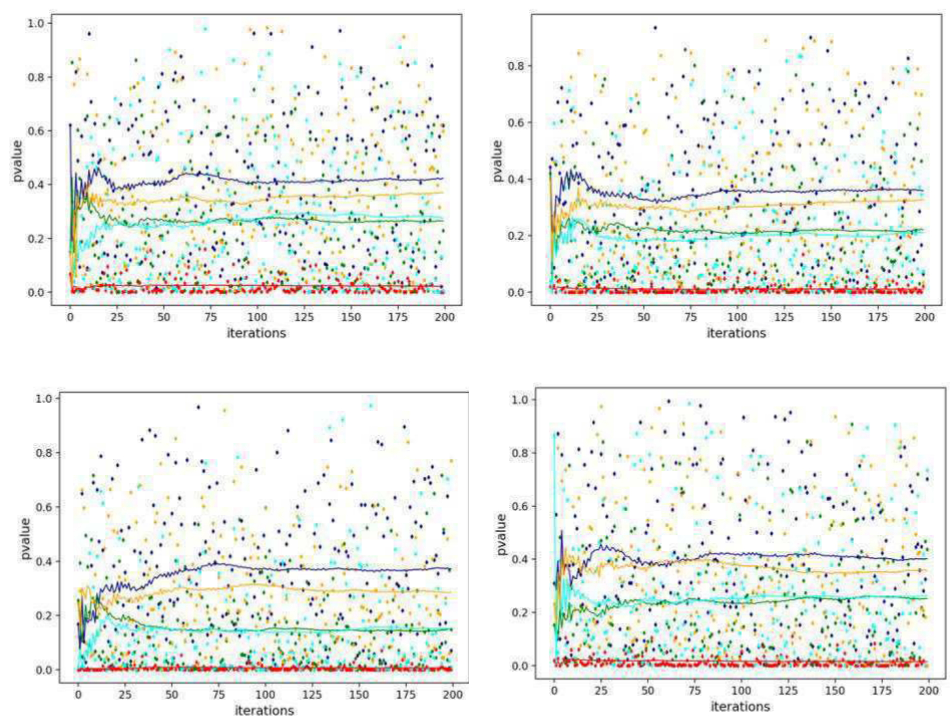

Figure14: Parametric Bootstrapping of p-value with Kolmogorov-Smirnov goodness of fit test. Upper left: p-values of fitting distribution on coarse-grained ω_1. Upper right: p-values of fitting distribution on coarse-grained ω_2. Lower left: p-values of fitting distribution on coarse-grained ω_3. Lower right: p-values of fitting distribution on coarse-grained ω_4; (blue: p-values from t-students' statistics, yellow: p-values from Laplace statistics, green: p-values from Cauchy statistics, red: p-values from normal statistics, cyan: p-values from Pearson statistics).

Appendix B: Conjugate prior of normal distribution

Let $X_1, \dots, X_n$ be n observations sampled from a probability density $p(X|\sigma^2)$ with σ^2 a random variable and $p(X|\sigma^2)$ represents the conditional probability density of X conditioned on σ^2. In contrast we write $p_{\sigma^2}(X)$ if we consider σ^2 as a deterministic value.
By Bayes' theorem, the posterior distribution can be written as:

$$p(\sigma^2|X_1, \dots, X_n) = \frac{p(X_1,\dots,X_n\,|\sigma^2)\pi(\sigma^2)}{p(X_1,\dots,X_n)} = \frac{\mathcal{L}_n(\sigma^2)\pi(\sigma^2)}{c_n} \propto \mathcal{L}_n(\sigma^2)\pi(\sigma^2) \quad (5)$$

Where $\mathcal{L}_n(\sigma^2) = \prod_{i=1}^{n} p(X_i|\sigma^2)$ is the likelihood function and:

$c_n = p(X_1, \dots, X_n) = \int p(X_1, \dots, X_n|\sigma^2)\,\pi(\sigma^2)d\sigma^2 = \int \mathcal{L}_n(\sigma^2)\pi(\sigma^2)d\sigma^2$ is the normalizing constant, which is also called the evidence.

A prior distribution is conjugate if it is closed under sampling. That is, if P is a family of prior distributions, and for each σ^2, we have a distribution $p(.|\sigma^2) \in \mathcal{F}$ over a sample space χ. Then, if the posterior:

$$p(\sigma^2|x) = \frac{p\left(x\middle|\sigma^2\right) * \pi(\sigma^2)}{\int p\left(x\middle|\sigma^2\right)\pi(\sigma^2)d\sigma^2} \quad (6)$$

satisfies $p(.|\sigma^2) \in P$, we say that the family P is conjugate to the family of sampling distributions $\mathcal{F}$. In order for this to be a meaningful notion, the family P should be sufficiently restricted, and is typically taken to be a specific parametric family.
We can characterize the conjugate priors for general exponential family models. Suppose that $p(.|\sigma^2)$ is a Gaussian model with known μ, so that the free parameter is the variance σ^2. The likelihood function is:

$$p(x_1, \dots, x_n|\sigma^2) \propto (\sigma^2)^{-n/2} exp\left(-\frac{1}{2\sigma^2}\sum_{i=1}^{n}(X_i - \mu)^2\right) = (\sigma^2)^{-n/2} exp\left(-\frac{n}{2\sigma^2}\overline{(X - \mu)^2}\right) \quad (7)$$

where

$$\overline{(X - \mu)^2} = \frac{1}{n}\sum_{i=1}^{n}(X_i - \mu)^2$$

The conjugate prior is an inverse Gamma distribution. Recall that σ^2 has an inverse gamma distribution with parameters α and β in case $1/\sigma^2 \sim Gamma(\alpha, \beta)$; the density takes the form:

$$\pi_{\alpha,\beta}(\sigma^2) \propto (\sigma^2)^{-(\alpha+1)} e^{-\beta/\sigma^2} \quad (8)$$

With this prior, the posterior distribution of σ^2 is given by:

$$\sigma^2 \mid X_1, \dots, X_n \sim InvGamma\left(\alpha + \frac{n}{2}, \beta + \frac{n}{2}\overline{(X - \mu)^2}\right) \quad (9)$$

Appendix C: Standard&Poor500 time series studied on different time scale

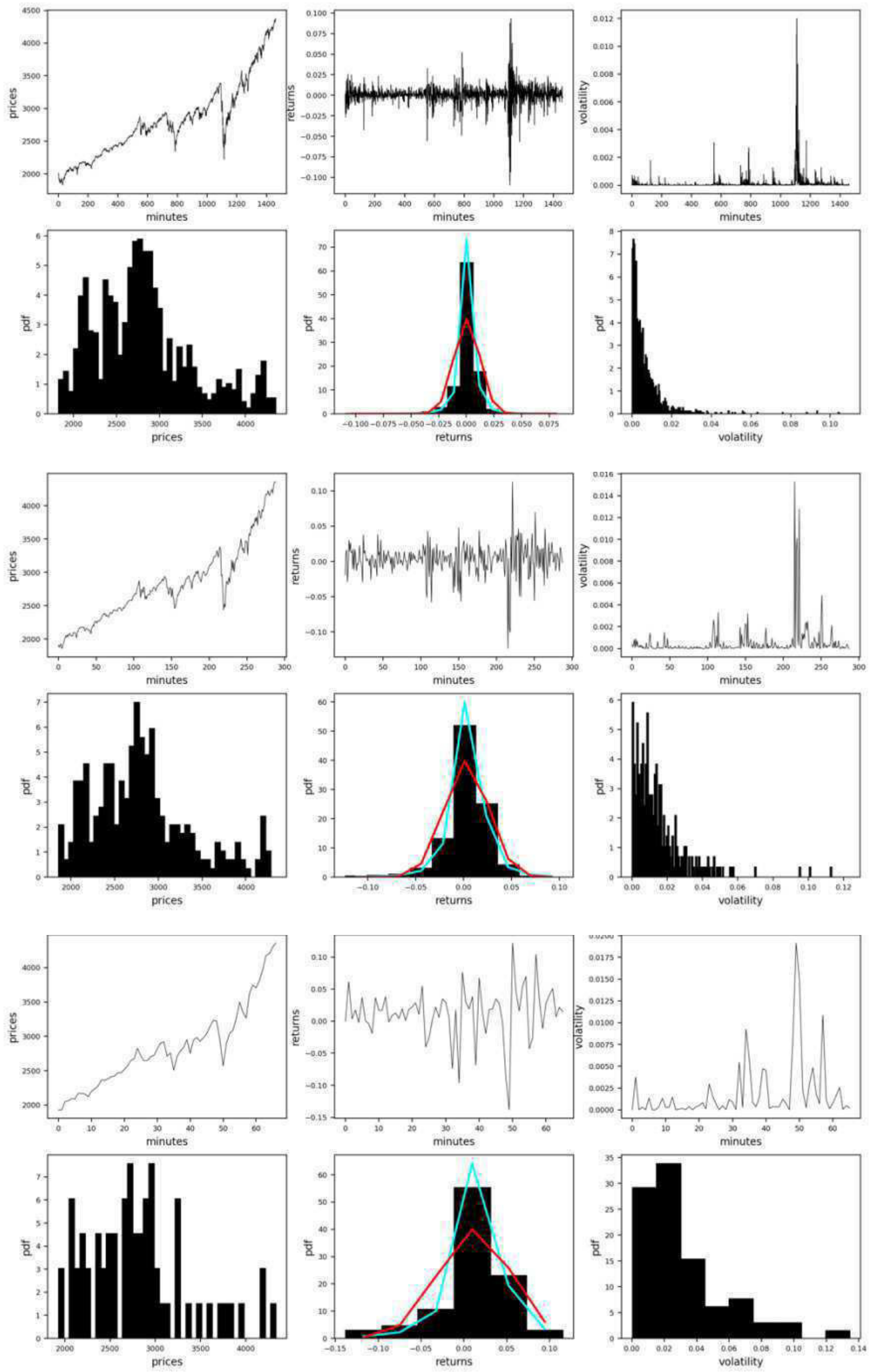

Figure15: Standard&Poor500 time series from January 01, 2016 to July 16, 2021. From upper to lower: time frame = daily, weekly, monthly. The cyan color line is a fit of t-students distribution. The red color line is a fit of normal distribution.

Appendix D: Statistical outcomes from distributions Goodness fit

Table10: Parameters of fitting distribution. Upper table: fitting parameters on data from daily time frame. Middle table: fitting parameters on data from weekly time frame. Lower table: fitting parameters on data from monthly time frame.

Daily data	2016	2017	2018	2019	2020	2021
IGa(x,α,β)	α:1.95, β:3.987e-05	α:1.93, β:1.018e-05	α:1.973, β:4.23e-05	α:1.955, β:7.33e-05	α:0.096, β:2.25e-07	α:1.91, β:7.074e-05
LN(x,μ,σ)	μ:-1.30e-08 σ: 2.343	μ:-2.297e-09 σ: 2.486	μ:-6.468e-09 σ: 2.509	μ:-2.505e-08 σ: 2.33	μ:-529e-09 σ: 2.65	μ:-6.23e-08 σ: 2.16
Ga(x,α,β)	α:0.17, β:0.8085	α:0.11, β:0.7506	α:0.067, β: 0.815	α:0.166, β:0.815	α:0.21, β:197.61	α:0.088, β:0.64

Weekly data	2016	2017	2018	2019	2020	2021
IGa(x,α,β)	α:1.88, β:0.00025	α:2.01, β:8.56e-05	α:1.90, β:0.00026	α:1.36, β:0.00026	α:0.51, β:4.023e-05	α:1.095, β:0.00017
LN(x,μ,σ)	μ:-3.253e-07 σ: 2.187	μ:-3.695e-05 σ: 0.678	μ:-2.29e-07 σ: 2.18	μ:-1.069e-06 σ: 2.015	μ: 1.744e-07 σ:2.471	μ:-2.95e-06 σ: 1.647
Ga(x,α,β)	α:0.53, β:2689.43	α:0.76, β:1/6.95e-05	α:0.42, β:805.03	α:0.48, β:1/ 0.00084	α:0.258, β:87.32	α:0.495, β:1/0.00087

Monthly data	2016	2017	2018	2019	2020	2021
IGa(x,α,β)	α:2.54, β:0.00096	α:0.69, β:6.71e-05	α:1.60, β:0.0015	α:1.55, β:0.00101	α:1.097, β:0.0023	α:1.76, β:0.0011
LN(x,μ,σ)	μ:6.71e-08 σ: 8.14	μ:6.562e-07 σ: 6.252	μ:2.29e-06 σ: 6.873	μ: - 0.00075 σ: 0.618	μ:9.16e-05 σ: 1.77	μ:-0.00033 σ: 0.709
Ga(x,α,β)	α:0.34, β:1/0.00093	α:0.57, β:1/0.00096	α:0.64, β:1/0.0026	α:0.26, β:1/0.0012	α:0.668, β:1/0.0043	α:0.32, β:1/0.00046

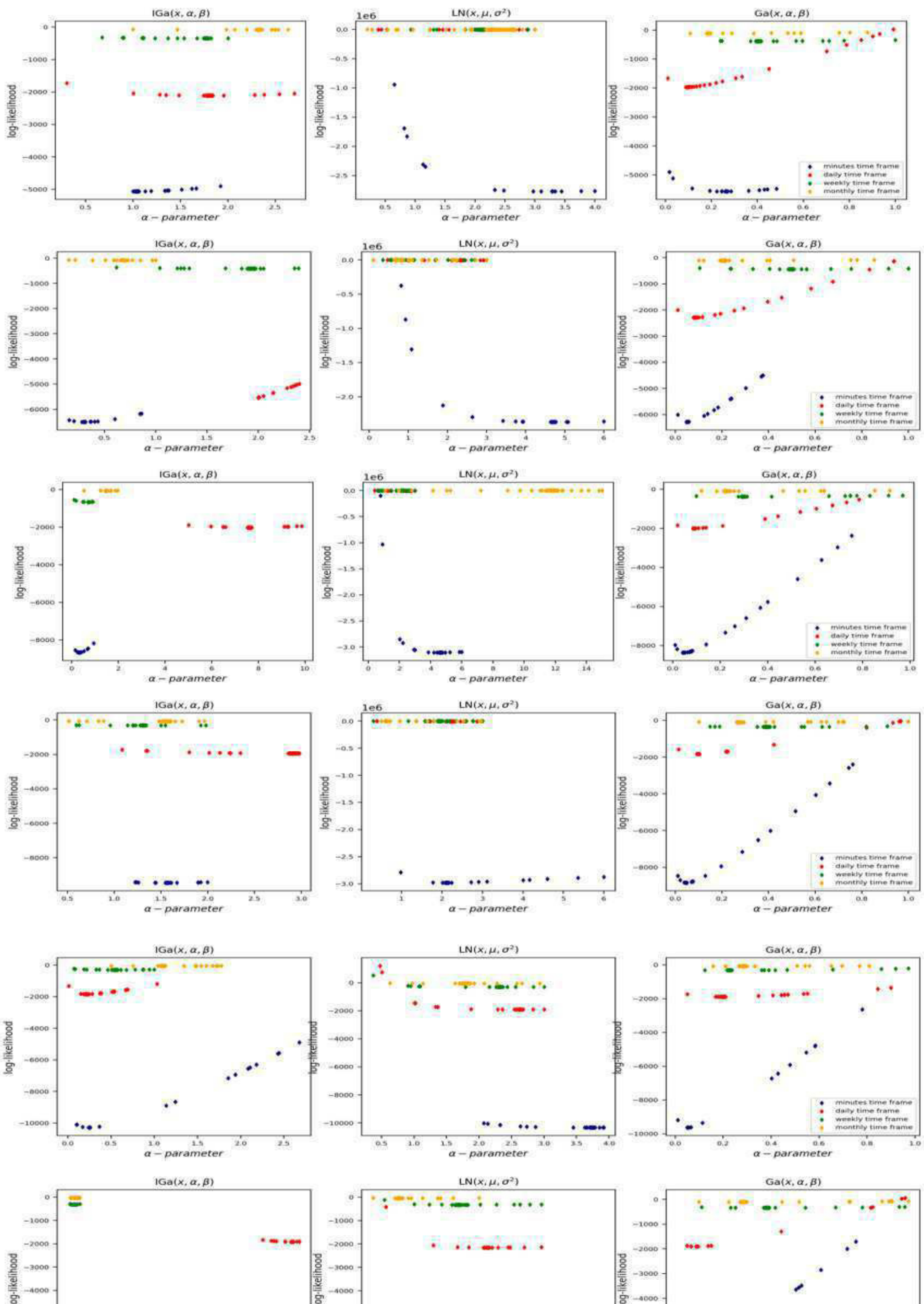

Figure16: Log-likelihood of Standard&Poor500. Each row corresponds to the log-likelihood regarding a respective year, starting on the top from 2016 and finish lower in 2021. Left graph: Log-likelihood for estimating IGa parameters. Middle graph: Log-likelihood for estimating LN parameters. Right graph: Log-likelihood for estimating Ga parameters

Table11: Distribution's fitting comparison with sum of squared errors methodology for the year 2017 to 2021 and on different time frames. The distribution model that fit the simulated data with the lowest SSE should be preferred.

Year 2017	**minutes**	**daily**	**weekly**	**monthly**
Best fit distributions	**LN(x,μ,σ)**	**LN(x,μ,σ)**	**Ga(x,α,β)**	**Ga(x,α,β)**
SSE from LN	**2.43e+09**	**2.42e+09**	4.51e+09	8.28e+07
SSE from IGa	2.55+09	3.11e+10	3.93e+09	7.66e+07
SSE from Ga	2.55e+09	2.37e+10	**2.47e+09**	**7.60e+07**
p-value	0.476	0.489	0.552	0.687

Year 2018	**minutes**	**daily**	**weekly**	**monthly**
Best fit distributions	**LN(x,μ,σ)**	**IGa(x,α β)**	**LN(x,μ,σ)**	**Ga(x,α,β)**
SSE from LN	**5.00e+08**	1.19e+08	**1.43e+07**	9.01e+06
SSE from IGa	5.51e+08	**9.82e+07**	1.00e+08	1.05e+07
SSE from Ga	5.54e+08	3.57e+08	2.48e+07	**8.74e+06**
p-value	0.10	0.359	0.499	0.703

Year 2019	**minutes**	**daily**	**weekly**	**monthly**
Best fit distributions	**LN(x,μ,σ)**	**LN(x,μ,σ)**	**LN(x,μ,σ)**	**IGa(x,α β)**
SSE from LN	**1.8326e+09**	**3.50e+07**	**2.23e+07**	4.69e+07
SSE from IGa	1.83296e+09	7.44e+07	3.87e+07	4.45e+07
SSE from Ga	1.83293e+09	3.08e+08	2.26e+07	**5.57e+07**
p-value	0.058	0.507	0.507	0.738

Year 2020	**minutes**	**daily**	**weekly**	**monthly**
Best fit distributions	**LN(x,μ,σ)**	**LN(x,μ,σ)**	**IGa(x,α β)**	**Ga(x,α,β)**
SSE from LN	**9.50e+08**	**1.02e+07**	7.01e+05	1.85e+06
SSE from IGa	9.77e+08	2.23e+07	**2.96e+05**	2.06e+06
SSE from Ga	9.76e+08	1.76e+07	5.58e+06	**1.81e+06**
p-value	0.149	0.555	0.523	0.647

Year 2021	**minutes**	**daily**	**weekly**	**monthly**
Best fit distributions	**LN(x,μ,σ)**	**LN(x,μ,σ)**	**IGa(x,α β)**	**Ga(x,α,β)**
SSE from LN	**4.79e+11**	**3.64e+07**	6.93e+06	2.39e+08
SSE from IGa	5.36e+11	7.29e+08	**6.42e+06**	2.37e+08
SSE from Ga	5.35e+11	7.49e+08	6.58e+06	**2.35e+08**
p-value	0.132	0.496	0.522	0.443

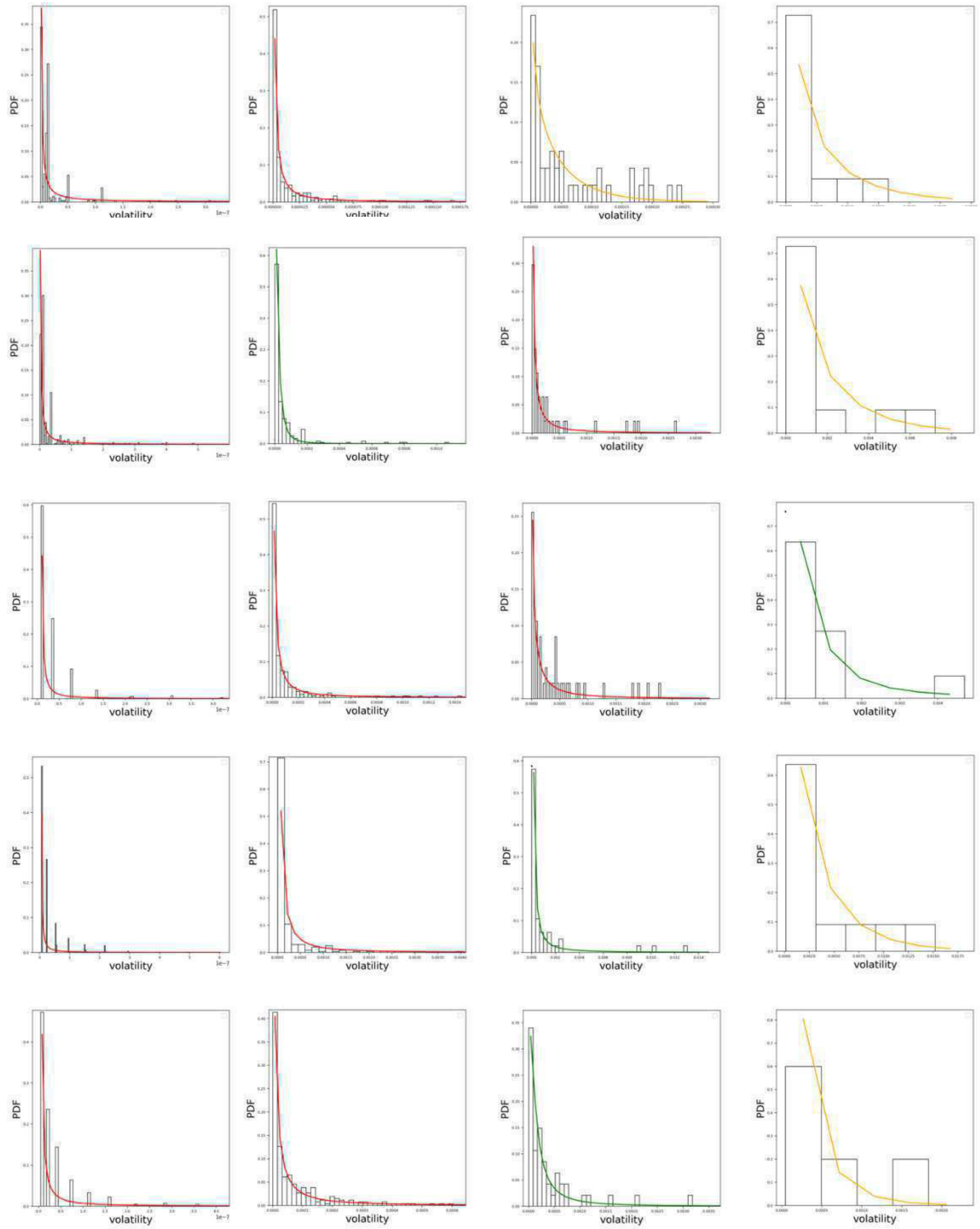

Figure17: Empirical distribution plotted against best fit distribution. Red line corresponds to LN distribution, green line corresponds to IGa distribution and yellow line corresponds to Ga distribution. From left to right, time frame = minutes, daily, weekly, monthly. From upper to lower, year start from 2017 to 2021. We observe a transition of statistics from high to low frequency, from LN to Ga.

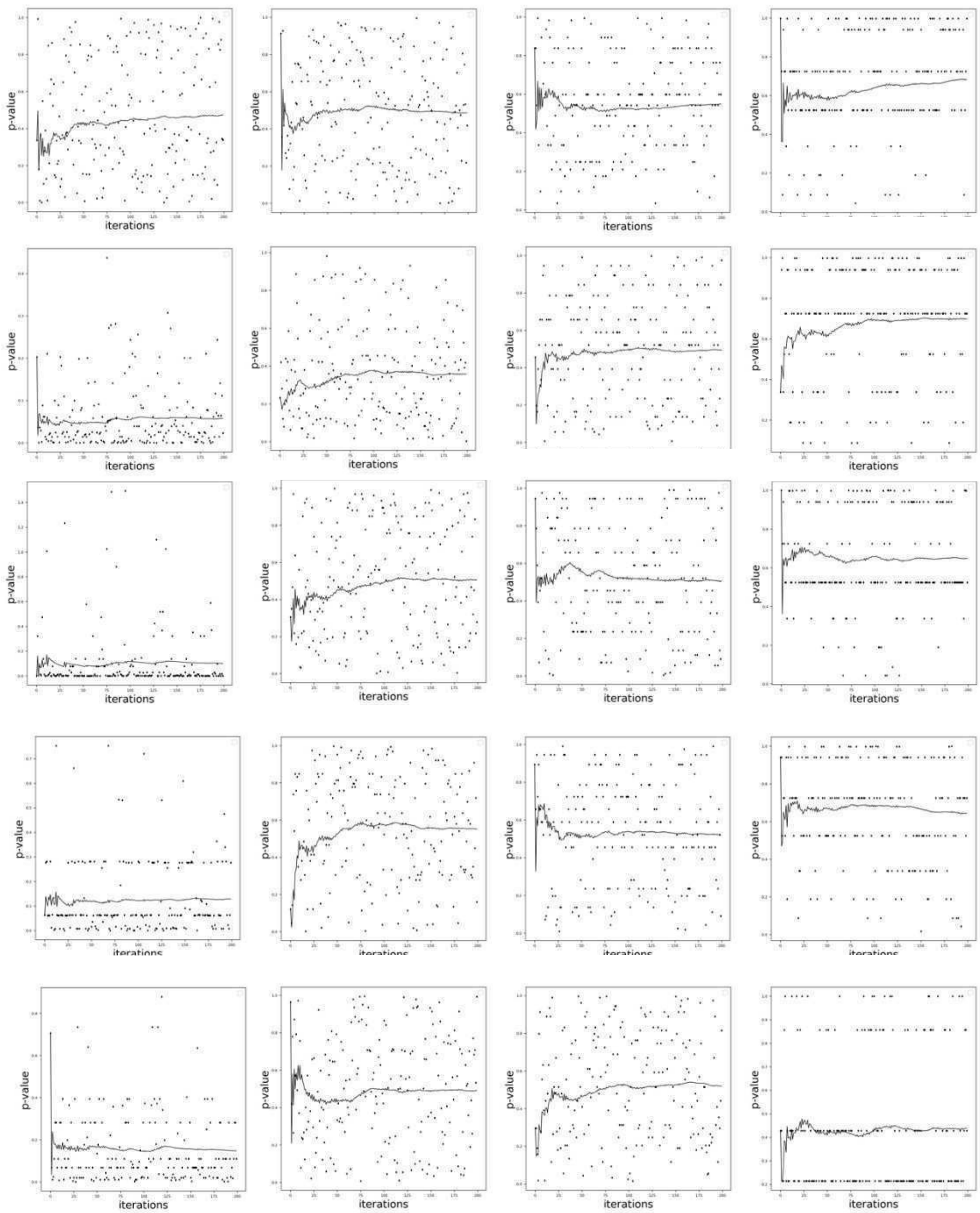

Figure18: Parametric Bootstrapping of p-value with Kolmogorov-Smirnov goodness of fit test regarding the best fit distribution. From left to right, time frame = minutes, daily, weekly, monthly. From upper to lower, year start from 2017 to 2021.